07

Semi-flexible photovoltaic modules based on silicon HJT cells

© S.A. Yakovlev,[1,2] I.Yu. Dmitriev,[1] M.Yu. Mikhailov,[1] K.V. Emtsev,[1,2] A.S. Abramov,[1,2] E.I. Terukov[1,2]

[1] R&D Center of Thin Film Technologies in Energetics,
194064 St. Petersburg, Russia
[2] Ioffe Institute,
194021 St. Petersburg, Russia
e-mail: S.Yakovlev@hevelsolar.com

Received May 15, 2024
Revised June 20, 2024
Accepted June 27, 2024

Semi-flexible and lightweight photovoltaic modules based on silicon heterojunction solar cells interconnected by Smart Wire film-wire electrode have been developed. Reliability of such module design to environmental stress factors has been studied: damp heat and thermocycling tests as per GOST R 56980.2 (IEC 61215-2:2016) — 2020. It is shown that one of the main degradation mechanisms of the module characteristics under high temperature and humidity is the corrosion of the film-wire electrodes. Different wire coatings of the electrodes were tested for its climatic resistance. It has been established that wire with SnBiAg coating is more resistant to moisture than wire with InSn coating. The resistance of the semi-flexible modules to hot spot heating effects before and after hail impact cell damage has been investigated. The effectiveness of the Smart Wire contacting technology against hail impact has been shown and the necessity of controlling the number of series-connected solar cells to minimize the risks of critical local overheating in semi-flexible modules has been demonstrated.

Keywords: semi-flexible photovoltaic modules, heterostructure silicon solar elements, Smart Wire contacting technology, reliability climate testing, local overheating, hail impact resistance.

DOI: 10.61011/TP.2024.10.59364.173-24

Introduction

The development of semi-flexible photovoltaic modules (PVM) based on silicon cells is one of the growing research trends in photovoltaics [1–5]. Such PVMs have found wide application in electrical plants of ground transport, shipbuilding, aviation, and solar power systems integrated into buildings (roofs, facades) [6–9]. In semi-flexible PVMs, the front glass is replaced by a transparent polymer sheet, which gives them a number of advantages: first, the specific weight of standard glass/back sheet PVMs is $\sim 12\,kg/m^2$, while the specific weight of semi-flexible PVMs is much lower and varies, depending on the design, from 1.5 to $3\,kg/m^2$; second, such PVMs may be bent to a certain extent, which enables their application on surfaces with a significant curvature, such as car roofs or boat hulls; third, the dimensions of semi-flexible PVMs do not depend on the glass size, allowing one to alter their shape freely (cut corners, round off, etc.) and fill the effective surface as efficiently as possible. In addition, a variety of fasteners are available for semi-flexible PVMs, which makes them convenient to install and use in various operating conditions. They may be secured with double-sided adhesive tape, sealing compounds, eyelets and screws, clasps, fabric hook-and-loop fasteners, etc. However, in addition to offering a number of advantages, semi-flexible PVMs have certain disadvantages. Since glass is replaced with a polymer sheet, they are more sensitive to mechanical and climatic influences, which shortens their lifetime [10–12].

In the present study, we report on the design of semi-flexible PVMs with protective polymer sheets based on polyethylene terephthalate (PET) and silicon heterojunction photovoltaic converters (HJT PVCs) interconnected by a SmartWire (SW) film-wire electrode (FWE) [13,14]. This design has passed climatic tests as per GOST R 56980.2 (IEC 61215-2:2016) — 2020. The influence of the SW wire type on reliability of semi-flexible PVMs was examined additionally, and their resistance to local hot spot heating before and after exposure to hail impacts was investigated.

1. Materials and methods

Semi-flexible PVMs for tests were fabricated based on HJT PVCs $157.35 \times 157.35\,mm$ in size and $130\,\mu m$ in thickness produced by Hevel Group [15]. HJT PVCs with an efficiency higher than 23% were connected in series into a string with the use of an SW FWE and a copper busbar with a cross section of $6 \times 0.3\,mm$ coated with $Sn_{96.5}Ag_{3.5}$ solder $14-20\,\mu m$ in thickness. The FWE was a double-layer polymer film (PET $12\,\mu m$ + polyolefin adhesive layer $65\,\mu m$) with 18 copper wires $250\,\mu m$ in diameter fused into it. These wires were coated with a layer of solder based on molten $In_{52}Sn_{48}$ (InSn) or $Sn_{42}Bi_{57}Ag_1$ (SnBiAg) with a thickness of $5-7\,\mu m$ (Fig. 1). The contact between wires and the silver current-collecting

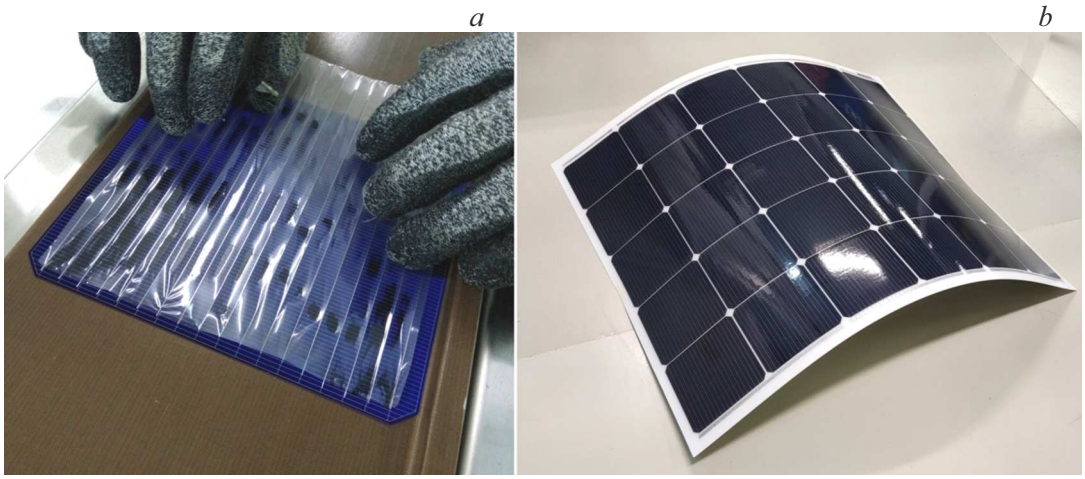

Figure 1. *a* — Manual gluing of an SW FWE to HJT PVCs on a heating table performed to produce a chain of series-connected PVCs; *b* — photographic image of a semi-flexible PVM containing 6 × 5 HJT PVCs.

Table 1. Degradation of electrical parameters of semi-flexible PVMs after high-temperature and high-humidity tests

Parameters	PVM with InSn wire		PVM with SnBiAg wire		
Test conditions	Initial	After 1000 h	Initial	After 1000 h	After 1700 h
I_{sc}, A	8.69	8.48	8.87	8.77	8.76
U_{oc}, V	21.98	21.86	22.08	22.03	22.04
I_{mpp}, A	8.20	7.98	8.46	8.36	8.30
U_{mpp}, V	18.40	17.70	18.52	18.33	18.29
P_{mpp}, W	150.93	141.20	156.63	153.19	151.77
FF,%	79.01	76.17	80.01	79.32	78.60
Power degradation, $\Delta P/P_{init}$, %	–	∼ 6.4%	–	∼ 2.2%	∼ 3.1%

Note. Here, I_{sc} is the short-circuit current, U_{oc} is the open-circuit voltage, I_{mpp} and U_{mpp} are the current and voltage values at the point of maximum power, P_{mpp} is the maximum PVM power, and FF is the fill factor.

grid of HJT PVCs was established by soldering in the course of PVM lamination. A transparent/white PET-based polymer sheet with a thickness of 420 μm and a water vapor transmission rate (WVTR) below 0.65 g/(m^2·day) was used for front/back protection; a thermoplastic polyolefin film 450 μm in thickness with a melting point of 130°C served as the encapsulant. The specific weight of this PVM structure was 2.1 kg/m^2.

Semi-flexible PVMs containing 2 × 5, 2 × 6, and 6 × 5 HJT PVCs were fabricated with the use of a laboratory laminator (Burkle GmbH). The current–voltage characteristics (IV) of samples were measured with a cetisPV tester (h.a.l.m. elektronik GmbH) under standard conditions (1000 W/m^2, AM 1.5AM, 25°C). Electroluminescence (EL) images were obtained using an MBJ Solutions SM-EL-lab inspection system.

PVM reliability tests were carried out in accordance with GOST R 56980.2 (IEC 61215-2:2016) — 2020. These included a damp heat test, thermal cycling, a hot spot resistance test, and a hail test. In climatic tests, PVMs containing 6 × 5 HJT PVCs were suspended in the chamber by four attachment points. To test the resistance to hot spot heating, PVMs containing 2 × 5 and 2 × 6 HJT PVCs were glued with double-sided adhesive tape to a heat-insulating sandwich panel to simulate the actual operating conditions of such PVMs. A custom-built test setup, which launched ice balls with a diameter of 25 mm at a velocity of 23 m/s, was used for the hail test. The samples were secured to a rigid base with thin double-sided adhesive tape.

2. Results and discussion

Two semi-flexible PVMs containing 6 × 5 HJT PVCs with different (InSn and SnBiAg) solder layers on SW FWE wires were fabricated for damp heat testing (85°C / 85% (rel. humidity)). The results of IV and EL measurements of PVMs before and after the test are presented in Table 1 and Fig. 2. It is evident that the PVM with InSn wire failed the test, since its power degradation was 6.4% after 1000 h, while the permissible level specified in the standard is only 5%. At the same time, the PVM with SnBiAg

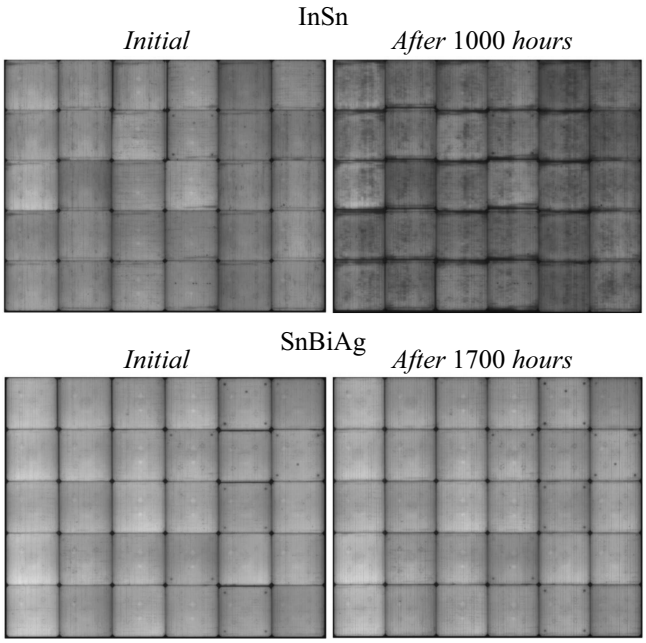

Figure 2. Electroluminescence of semi-flexible PVMs prior to and after damp heat tests

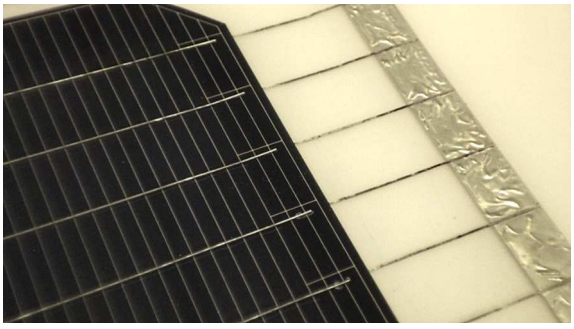

Figure 3. InSn wire corrosion within a PVM after 1000 h of damp heat testing.

wire demonstrated fine resistance to moisture at elevated temperatures with a power degradation of just 3.1% even after 1700 h.

The EL images of the PVM with InSn wire revealed darkening throughout the entire area of cells after 1000 h of testing, which indicates a local increase in contact resistance. Visual inspection of the PVM showed that InSn wires were corroded (Fig. 3), which led to deterioration of the contact between the wire and the current-collecting metallized grid on the PVC surface. SnBiAg wires showed no signs of corrosion after 1700 h of testing.

Another two semi-flexible PVMs containing 6×5 HJT PVCs with InSn and SnBiAg wires were fabricated for thermal cycling within the temperature range from -40 to $+85^{\circ}$C. The results of IV and EL measurements of PVMs before and after the test are presented in Table 2 and Fig. 4. Both PVMs passed the required 200 thermal cycles. In fact, the tests were extended further to 350 cycles. The power degradation of the PVMs with SnBiAg and InSn wires was approximately 3.0% and 4.1%, respectively.

Darkening was observed in the EL images for both PVMs after 350 test cycles, which is attributable, first, to partial loss of contact between the wires and the metallization grid and, second, to breaking of SW FWE wires in the gaps between PVCs in the string (Fig. 5).

One of the critical problems arising in practical application of semi-flexible PVMs is local hot spot overheating due to partial shading and/or PVC damage (the „hot spot“ effect [16–18]). Since semi-flexible PVMs are usually attached to a certain surface, heat dissipation is impeded. Therefore, the operating temperature and the temperature under the conditions of partial shading of such PVMs are higher than those of PVMs mounted in a standard fashion. In addition, the substitution of glass with a polymer sheet makes semi-flexible PVMs more vulnerable to mechanical damage and PVC cracking, which may result in strong point heating and even burn-through of PVMs in the case of partial shading.

Semi-flexible PVMs containing 10 (2×5) and 12 (2×6) series-connected HJT PVCs with an SW FWE with SnBiAg wires were fabricated in order to examine the influence of local overheating in the partial shading mode. The PVMs were secured to a 65-mm-thick heat-insulating sandwich panel made of extruded polystyrene foam to simulate the worst case of heat dissipation. The test was performed outdoors in controlled conditions as per GOST R 56980.2 (IEC 61215-2 : 2016) — 2020. The temperature of the PVMs on the sandwich panel in the operating mode without shading was approximately 70°C.

It was established experimentally that the temperature of a semi-flexible PVM reaches its maximum in a test with PVC shading by 15–20%. Under these conditions, the PVM with 2×6 PVCs was heated to $\sim 140^{\circ}$C, and the PVM with 2×5 PVCs was heated to $\sim 120^{\circ}$C. The IV and EL images recorded after 3 h of testing revealed an insignificant power degradation ($\sim 0.4\%$) and no changes in EL for both PVMs. However, the PVM with 2×6 PVCs was severely deformed with a breach of tightness in the shading area, while visual inspection of the PVM with 2×5 PVCs revealed no such deformation (Fig. 6).

The heavy deformation of the PVM with 2×6 PVCs is attributable to the fact that its temperature during testing exceeded the melting point of the encapsulant (130°C). When the temperature reached 140°C, the thermoplastic polyolefin film transitioned to a liquid state, and this led to PVM deformation, since a rigid substrate (in the case of standard PVMs, glass) was lacking. Thus, in the considered design of semi-flexible PVMs, the number of series-connected PVCs per a single bypass diode should be limited to 10.

Mechanical strength is another critical issue for semi-flexible PVMs. The resistance to mechanical impact of a PVM containing 2×5 HJT PVCs was assessed via a hail test. To minimize damage, the PVM was secured

Table 2. Degradation of electrical parameters of semi-flexible PVMs after thermal cycling

Parameters	PVM with InSn wire			PVM with SnBiAg wire		
Test conditions	Initial	After 200 cycles	After 350 cycles	Initial	After 200 cycles	After 350 cycles
I_{sc}, A	8.80	8.52	8.62	8.88	8.84	8.82
U_{oc}, V	21.99	21.92	21.95	22.07	22.07	22.08
I_{mpp}, A	8.31	8.11	8.14	8.48	8.41	8.35
U_{mpp}, V	18.37	18.15	18.00	18.48	18.38	18.19
P_{mpp}, W	152.69	147.12	146.49	156.65	154.66	151.96
FF, %	78.94	78.78	77.40	79.95	79.28	78.03
Power degradation, $\Delta P/P_{init}$, %	–	~ 3.6	~ 4.1	–	~ 1.3	~ 3.0

Note. Here, I_{sc} is the short-circuit current, U_{oc} is the open-circuit voltage, I_{mpp} and U_{mpp} are the current and voltage values at the point of maximum power, P_{mpp} is the maximum PVM power, and FF is the fill factor.

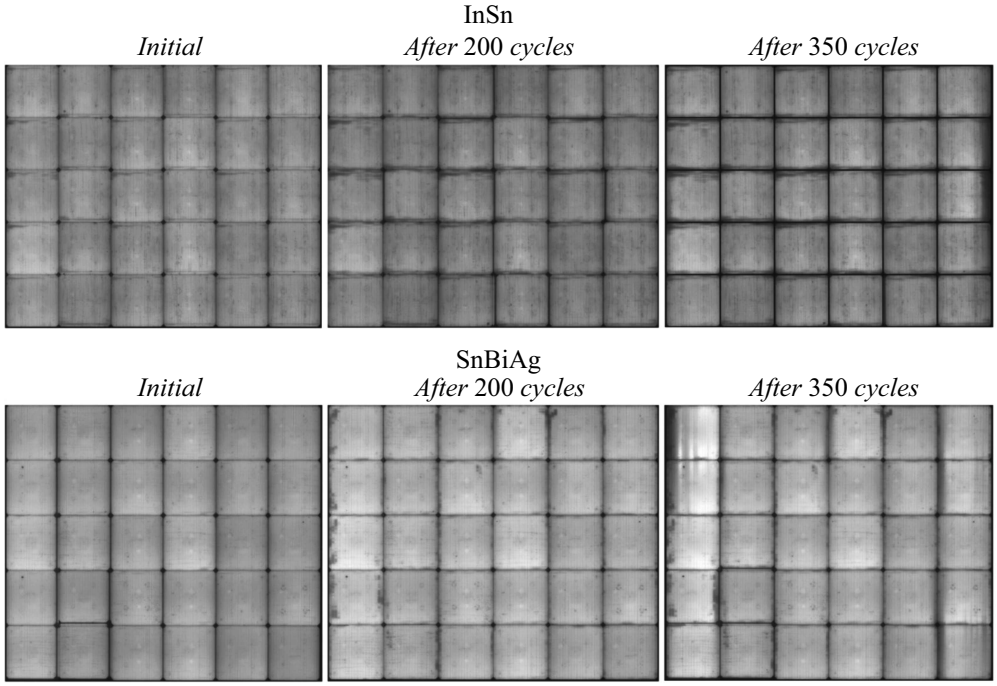

Figure 4. Images of EL of semi-flexible PVMs before and after thermal cycling.

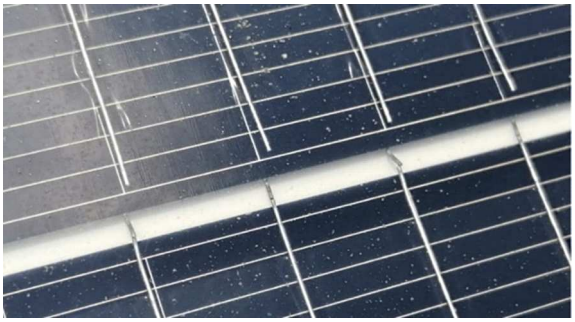

Figure 5. Breaking of SW FWE wires in the gaps between PVCs after 350 thermal cycles.

with thin double-sided adhesive tape to a rigid surface in such a way that no air gap remained between it and the surface [11]. The PVM power degradation after several hail impacts events was 0.9%, and no visible damage was detected. Therefore, according to the criteria specified in the standard, the PVM has passed the test. However, it should be noted that point damages (isolated local cracks) were observed on individual PVCs after the test (Fig 7).

The effect of hail damage to PVCs and on the possible subsequent local PVM overheating at the damaged site was also investigated in the present study. The damaged PVC was shaded by 15–20% for this purpose. The PVM temperature in the region of the shaded PVC was ~ 120–130°C. Control EL measurements revealed an

Figure 6. Deformation of a semi-flexible PVM containing 2 × 6 PVCs and lack of deformation of a PVM containing 2 × 5 PVCs after hot spot testing.

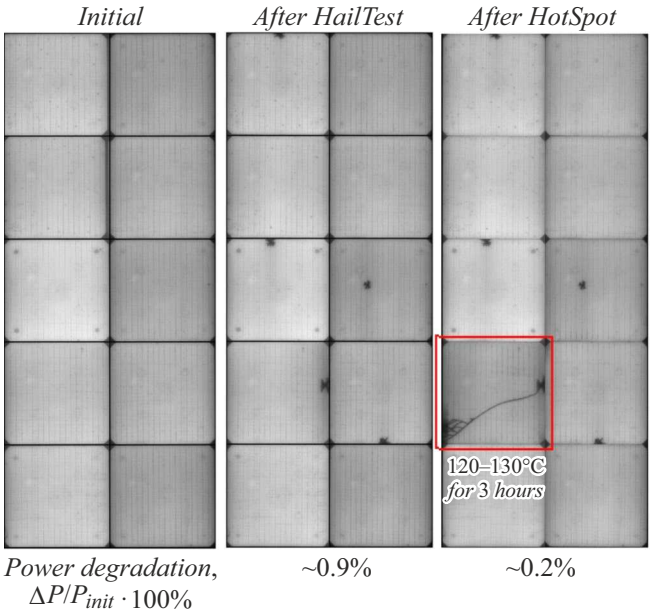

Figure 7. Results of tests of a semi-flexible PVM containing 2 × 5 PVCs for resistance to hail impacts and subsequent hot spot heating.

extended crack originating at the site of point hail damage to the PVC (Fig. 7). Thus, PVC damage may enhance the effect of local hot spot overheating, potentially affecting the reliability of the PVM structure.

Conclusion

A design of semi-flexible lightweight PVMs based on HJT PVCs connected via the SmartWire contacting technology was proposed. This design has passed a damp heat test in the scope exceeding significantly the one specified in the standard (more than 1500 h) and a thermal cycling test (more than 350 h) with a power degradation of just ∼ 3%.

It was found that SW FWE wires with SnBiAg coating should be used to ensure reliable operation of a semi-flexible PVM, since they demonstrate a higher resistance to corrosion under the influence of moisture than wires with InSn solder. It was also determined that the optimum PVM design is a structure with no more than 10 PVCs per bypass diode, since the use of a greater number of cells carries the potential risk of local PVM overheating above the melting point of the encapsulant, which may lead to deformation of the PVM and its failure in the partial shading mode.

It was noted that the SmartWire multi-wire contacting system helps reduce the PVM power degradation after hail strikes to insignificant levels, but continued operation of a semi-flexible PVM with cracked PVCs increases the risk of its local overheating. These results are of significant importance for further improvement of semi-flexible PVMs and their application in practice.

Conflict of interest

The authors declare that they have no conflict of interest.

References

[1] T. Tachibana, K. Shirasawa, K. Tanahashi. Solar Energy Materials and Solar Cells, **262**, 11254 (2023). DOI: 10.1016/j.solmat.2023.112541
[2] T.M. Hammam, B. Alhalaili, M.S. Abd El-sadek, A.A. Abuelwafa. Sensors, **23**, 7995 (2023). DOI: 10.3390/s23187995
[3] J. Ulbikas, M. Rudzikas, P. Dubravskij, A.G. Ulyashin. Proceed. Intern. Conf. 37th EU PVSEC, Poster 4AV.2.29 (2020).
[4] N. Pervan, G.C. Eder, Y. Voronko, C. Ballif, F. Lisco, U. Desai, A. Derluyn, J. Govaerts, B. Luo, G. Oreski. Proceed. Inter. Conf. 40th EU PVSEC, Poster 3AV.1.12 (2023).
[5] H. Nussbaumer, M. Klenk, N. Keller. Proceed. Inter. Conf. 32th EU PVSEC, p. 56–60 (2016). DOI: 10.4229/EUPVSEC20162016-1BO.12.5
[6] A. Abramov, D. Andronikov, K. Emtsev, D. Orekhov, I. Shakhray, E. Terukov, E. Terukova, S. Yakovlev. Proceed. Inter. Conf. 35th EU PVSEC, p. 1227–1229 (2018). DOI: 10.4229/35thEUPVSEC20182018-5CV.1.34
[7] M.J. Park, S. Youn, K. Jeon, S.H. Lee, C. Jeong. Appl. Sci., **12**, 5011 (2022). DOI: 10.3390/app12105011

[8] B. Commault, T. Duigou, V. Maneval, J. Gaume, F. Chabuel, E. Voroshazi. Appl. Sci., **11**, 11598 (2021). DOI: 10.3390/app112411598
[9] G. Minak. J. Mar. Sci. Eng., **11**, 1519 (2023). DOI: 10.3390/jmse11081519
[10] S. Yakovlev, E. Schebet, K. Emtsev, D. Andronikov, A. Abramov, D. Orekhov, I. Shakhray. Proceed. Inter. Conf. 37th EU PVSEC, p. 1117–1119 (2020). DOI: 10.4229/EUPVSEC20202020-4AV.2.18
[11] S. Yakovlev, E. Schebet, K. Emtsev, D. Andronikov, A. Abramov, D. Orekhov, I. Shakhray. Proceed. Inter. Conf. 36th EU PVSEC, p. 1040–1041 (2019). DOI: 10.4229/EUPVSEC20192019-4AV.1.22
[12] F. Lisco, A. Virtuani, C. Ballif. Proceed. Inter. Conf. 37th EU PVSEC, p. 777–783 (2020). DOI: 10.4229/EUPVSEC20202020-4BO.11.5
[13] A. Faes, M. Despeisse, J. Levrat, J. Champliaud, N. Badel, M. Kiaee, Th. Söderström, Yu Yao, R. Grischke, M. Gragert, J. Ufheil, P. Papet, B. Strahm, B. Cattaneo, G. Cattin, Ya. Baumgartner, A. Hessler-Wyser, Ch. Ballif. Proceed. Inter. Conf. 29th EU PVSEC, p. 2555–2561 (2014). DOI: 10.4229/EUPVSEC20142014-5DO.16.3
[14] B. Strahm, D. Lachenal, D.L. Bätzner, W. Frammelsberger, B. Legradic, J. Meixenberger, P. Papet, G. Wahli, E. Vetter, M. Despeisse, A. Faes, A. Lachowicz, Ch. Allebé, P.-J. Alet, M. Bonnet-Eymard, Ch. Ballif, Yu Yao, Ch. Rychen, Th. Söderström, J. Heiber, G. Schiltges, S. Leu, J. Hiller, V. Fakhfouri. Proceed. Inter. Conf. 29th EU PVSEC, p. 467–471 (2014). DOI: 10.4229/EUPVSEC20142014-2BO.4.1
[15] A.S. Abramov, D.A. Andronikov, S.N. Abolmasov, E.I. Terukov. In *High-efficient low-cost Photovoltaics. Springer Ser. in Optical Sciences* (Springer, Cham, 2020), v. 140, p. 113–132. DOI: 10.1007/978-3-030-22864-4_7
[16] F. Li, W. Dong, W. Wu. Adv. Appl. Energy, **9**, 100118 (2023). DOI: 10.1016/j.adapen.2022.100118
[17] E. Özkalay, F. Valoti1, M. Caccivio1, A. Virtuani, G. Friesen, C. Ballif. EPJ Photovoltaics, **15**, 7 (2024). DOI: 10.1051/epjpv/2024001
[18] S. Deng, Z. Zhang, C. Ju, J. Dong, Z. Xia, X. Yan, T. Xu, G. Xing. Energy Procedia, **130**, 77 (2017). DOI: 10.1016/j.egypro.2017.09.399

Translated by D.Safin